"Nanostructured organic radical cathodes from self-assembled nitroxide-containing block copolymer thin films"

Hauffman, Guillaume ; Vlad, Alexandru ; Janoschka, T. ; Schubert, U. S. ; Gohy, Jean-François

Abstract

This contribution describes the formation of nanostructured thin film organic radical cathodes. First, the self-assembly of poly(styrene)-block-poly(2,2,6,6-tetramethylpiperidinyloxy-4-yl methacrylate) (PTMA-b-PS) diblock copolymers is detailed. In order to improve the nano-morphology of the immiscible PTMA and PS domains, the effect of thermal and solvent annealing is investigated. The formation of thin films with different morphologies such as cylindrical or lamellar nanostructures is observed depending on the processing conditions. The electrochemical properties of the nanostructured films are further investigated to assess the redox activity of the PTMA domains. Cyclic voltammetry of PTMA-b-PS diblock copolymers, either in dissolved or thin film supported configuration, confirms the reversible redox behavior of the nitroxide radical. Galvanostatic cycling of the thin film nanostructured cathodes reveals good capacity retention with fast charge/discharge response resulting from ef...

Document type : *Article de périodique (Journal article)*

Référence bibliographique

1
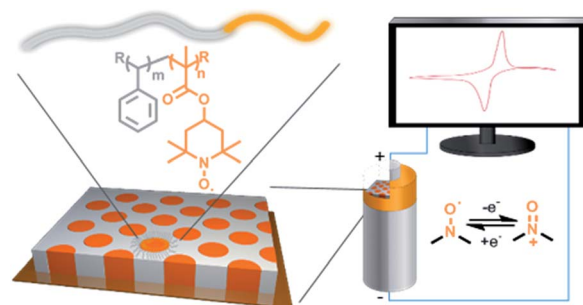
Nanostructured organic radical cathodes from self-assembled nitroxide-containing block copolymer thin films

G. Hauffman, A. Vlad, T. Janoschka, U. S. Schubert and J.-F. Gohy*

Nanostructured thin film organic radical cathodes have been prepared from poly(styrene)-*block*-poly(2,2,6,6-tetramethylpiperidinyloxy-4-yl methacrylate) diblock copolymers.

Please check this proof carefully. **Our staff will not read it in detail after you have returned it.**

Translation errors between word-processor files and typesetting systems can occur so the whole proof needs to be read. Please pay particular attention to: tabulated material; equations; numerical data; figures and graphics; and references. If you have not already indicated the corresponding author(s) please mark their name(s) with an asterisk. Please e-mail a list of corrections or the PDF with electronic notes attached - do not change the text within the PDF file or send a revised manuscript. Corrections at this stage should be minor and not involve extensive changes. All corrections must be sent at the same time.

Please bear in mind that minor layout improvements, e.g. in line breaking, table widths and graphic placement, are routinely applied to the final version.

We will publish articles on the web as soon as possible after receiving your corrections; **no late corrections will be made.**

Please return your **final** corrections, where possible within **48 hours** of receipt by e-mail to: materialsA@rsc.org

Queries for the attention of the authors

Journal: **Journal of Materials Chemistry A**

Paper: **c5ta05823f**

Title: **Nanostructured organic radical cathodes from self-assembled nitroxide-containing block copolymer thin films**

Editor's queries are marked like this... **1**, and for your convenience line numbers are inserted like this... 5

Please ensure that all queries are answered when returning your proof corrections so that publication of your article is not delayed.

Query Reference	Query	Remarks
1	For your information: You can cite this article before you receive notification of the page numbers by using the following format: (authors), J. Mater. Chem. A, (year), DOI: 10.1039/c5ta05823f.	
2	Please carefully check the spelling of all author names. This is important for the correct indexing and future citation of your article. No late corrections can be made.	
3	Do you wish to add an e-mail address for the corresponding author? If so, please supply the e-mail address.	
4	In "Fig. 6", a closing bracket has been inserted. Please check that this is correct.	
5	Ref. 14, 34, 39 and 41: Can these references be updated?	
6	Ref. 23: Please provide the journal title.	
7	Ref. 48: Please provide the last name for the 1st author.	
8	Ref. 48: Please provide the initial(s) for the 2nd author.	

PAPER

Nanostructured organic radical cathodes from self-assembled nitroxide-containing block copolymer thin films†

G. Hauffman,[a] A. Vlad,[a] T. Janoschka,[bc] U. S. Schubert[bc] and J.-F. Gohy*[a]

This contribution describes the formation of nanostructured thin film organic radical cathodes. First, the self-assembly of poly(styrene)-*block*-poly(2,2,6,6-tetramethylpiperidinyloxy-4-yl methacrylate) (PTMA-*b*-PS) diblock copolymers is detailed. In order to improve the nano-morphology of the immiscible PTMA and PS domains, the effect of thermal and solvent annealing is investigated. The formation of thin films with different morphologies such as cylindrical or lamellar nanostructures is observed depending on the processing conditions. The electrochemical properties of the nanostructured films are further investigated to assess the redox activity of the PTMA domains. Cyclic voltammetry of PTMA-*b*-PS diblock copolymers, either in dissolved or thin film supported configuration, confirms the reversible redox behavior of the nitroxide radical. Galvanostatic cycling of the thin film nanostructured cathodes reveals good capacity retention with fast charge/discharge response resulting from efficient charge and ion transfer as well as structural integrity. Such nanostructured organic radical cathodes provide opportunities for the fabrication of new generation nanostructured organic radical battery architectures.

Introduction

Due to an ever increasing demand for portable energy storage solutions, interest in organic radical batteries (ORBs) has burst out over the past decade.[1–3] Indeed ORBs, when compared to classical Li-ion batteries, do not need environmentally unfriendly and resources-limited transition metal compounds.[4] Moreover, ORBs are flexible, allow rapid charge/discharge processes and are based on potentially unlimited organic resources.[5]

In this context, this contribution focuses on organic radical cathode (ORC) materials based on poly(2,2,6,6-tetramethylpiperidinyloxy methacrylate) (PTMA). PTMA is a methacrylate bearing the 2,2,6,6-tetramethylpiperidinyloxy (TEMPO) moiety, a well-known stable persistent radical. The stable nitroxide present in the PTMA moiety presents a flat charge/discharge voltage profile at 3.6 V (*vs.* Li⁺/Li) with a theoretical capacity of 111 mA h g⁻¹. PTMA has been originally studied as a cathode material by Hasegawa *et al.*[6] in 2002 with further developments being proposed by Nishide and Suga.[7,8] PTMA is usually produced by free radical polymerisation (FRP) of 2,2,6,6-

tetramethylpiperidin-4-yl methacrylate (TMPM) followed by its oxidation to PTMA, and combined with conductive carbons and poly(vinylidene fluoride) (PVDF) to form the positive electrodes.[9–14] Besides PTMA, many other redox polymers have been considered as potential candidates for ORBs. In this respect, a wide variety of polymers bearing stable radicals is now available.[8,15–21] Moreover, by changing the surroundings of the nitroxide group *e.g.* by adding an electron-withdrawing group next to it, it is also possible to stabilise the n-type redox pair between the nitroxide radical and the aminoxyl anion, giving an organic radical anode.[22–26] The recent developments in controlled radical polymerization (CRP) techniques for the polymerization of TMPM have allowed the synthesis of well-defined PTMA with controlled molar mass and molar mass dispersity ($Đ_M$) lower than 1.5.[27–30] This advance has promoted the development of hybrid materials with PTMA grafted onto different surfaces such as silica nanoparticles, ITO substrates and carbon nanotubes.[31–34] Nishide *et al.* went further by grafting a block copolymer of TEMPO and glycidyl methacrylate onto an ITO substrate, leading to a polymer layer, with a thickness in the micrometre range, exhibiting a good storage capacity with good charge diffusivity.[35] This work provides a good example of the synergy that can be obtained using block copolymers with different properties. Another approach consists of using self-assembled block copolymers as templates in order to incorporate a TEMPO substituted ionic liquid, as demonstrated by Nishide *et al.*[36]

Surprisingly only a few reports have investigated the possibility opened by the CRP of TMPM for the formation of diblock

[a]Institute of Condensed Matter and Nanosciences (IMCN), Université catholique de Louvain, Place L. Pasteur, 1, Louvain-la-Neuve, Belgium
[b]Laboratory of Organic and Macromolecular Chemistry (IOMC), Friedrich Schiller University Jena, Humboldtstrasse 10, 07743 Jena, Germany
[c]Center for Energy and Environmental Chemistry Jena (CEEC Jena), Friedrich Schiller University Jena, Philosophenweg 7a, 07743 Jena, Germany
† Electronic supplementary information (ESI) available. See DOI: 10.1039/c5ta05823f

This journal is © The Royal Society of Chemistry 2015

J. Mater. Chem. A, 2015, **xx**, 1–7 | 1

copolymers with a stable nitroxide radical bearing block and the subsequent self-assembly study.

Concerning self-assembly in solution, amphiphilic block copolymers bearing stable nitroxyl radicals have been used to form micelles in aqueous media.[37] We previously reported the formation of electrochemically active micelles with a polystyrene (PS) insoluble core and PTMA soluble coronal chains using PTMA-*b*-PS diblock copolymers dissolved in commonly used Li-ion battery electrolytes.[38]

For self-assembly in thin films, Boudouris *et al.* reported the possibility to form thin films with tailored morphologies from polydimethylsiloxane-*block*-PTMA (PDMS-*b*-PTMA) diblock copolymers using solvent vapour annealing in CHCl$_3$.[39] In 2014, Nishide and Suga reported the synthesis of pendant radical- and ion-containing block copolymers. The self-assembled thin films exhibit different morphologies from spheres to inverse spheres and were used as an active layer in a diode-structured thin-film device, combining the redox-active radicals of one block to the charge-compensating ions of the other one.[40] More recently, Ober *et al.* reported the formation of cylindrical morphologies using block copolymers with a block of PTMA and different blocks of fluorinated and non-fluorinated methacrylates. They demonstrated that phase separation after thermal or solvent annealing only occurs for block copolymers with fluorinated blocks.[41] This contribution provides further advance with respect to control of PTMA-*b*-PS diblock copolymer self-assembly in thin films. PS was selected as a stable, electrochemically inert and battery electrolyte insoluble polymer block. We demonstrate the controlled acquisition of different morphologies from cylindrical to lamellar. We also confirm that the domain size depends on the molar mass of the used block copolymer. In the second part, the electrochemical properties of such thin films are investigated and we demonstrate the possibility to perform different electrochemical measurements directly on films thinner than 100 nm. The accordingly obtained thin films can be considered as a regular array of nanosized PTMA ORCs embedded in a supporting PS matrix.

Experimental part

Materials

N,*N*-Dimethylformamide (DMF, VWR, HyperSolv Chromanorm for HPLC), diethyl carbonate (DEC, Aldrich, 99%), acetonitrile (VWR, HyperSolv Chromanorm for HPLC), tetrahydrofuran (Aldrich, Normapur), silver nitrate (Belfolabo) and tetrabutylammonium perchlorate (TBAClO$_4$; Fluka) were used as received.

Instrumentation

Proton nuclear magnetic resonance (^{1}H NMR) spectra were acquired on a 300 MHz Bruker Avance II or on a 500 MHz Bruker Avance II. Molar masses (M_n) and molar mass dispersity ($Đ_M$) were measured on an Agilent size exclusion chromatography (SEC) system equipped with an Agilent 1100/1200 pump (25 °C; eluent: chloroform : triethylamine : 2-isopropanol (94 : 4 : 2); flow rate: 1 mL min^{-1}), an Agilent differential refractometer and two PSS SDV columns (beads 10 μm; porosity of column 1: 10 000 Å; porosity of column 2: 1000 Å). The calibration was

performed using polystyrene standards. Electron spin resonance (ESR) spectra were acquired on an EMXmicro CW-EPR spectrometer (Bruker, Germany) from powdered samples. The *SpinCount*™ software module was used for quantitative experiments. Rapid thermal annealing (RTA) was performed using a MILA-5000 Lamp Heating Unit from ULVAC. Atomic force microscopy (AFM) was performed on a Digital Instruments Nanoscope V scanning force microscope in tapping mode using NCL cantilevers (Si, 48 N m^{-1}, 330 kHz, Nanosensors). Cyclic voltammetry was performed using a CH Instruments potentiostat CHI 660B. Charge/discharge tests were performed using an ARBIN Instrument Battery Tester, BT-2043. A Pt-disk working electrode (CHI102), Pt wire counter electrode (CHI115) and dry Ag/Ag$^+$ non-aqueous reference electrode (CHI112) come from CH Instruments, Inc.

Polymer synthesis

PTMA-*b*-PS diblock copolymers were synthesised as previously described in ref. 28.

Degree of oxidation measurement

Electron spin resonance (ESR) spectra were acquired on an EMXmicro CW-EPR spectrometer (EMX micro EMM-6/1/9-VT control unit, ER 070 magnet, EMX premium ER04 X-band microwave bridge equipped with a EMX standard resonator, EMX080 power unit) by Bruker, Germany. Powdered samples (∼4 mg) were investigated at room temperature and data handling was done on the Bruker Xenon software package, version 1.1b86. For quantitative experiments the SpinCount™ software module was used and the SpinCount calculated as the average of three measurements. The degree of oxidation is determined by the ratio between the spin/mg value obtained by ESR and the NO/mg value theoretically calculated for a polymer with a theoretical degree of oxidation of 100%, considering that one nitroxide group corresponds to one electron spin in ESR.

Thin film preparation

Spin coating. Polymer thin films were spin-coated onto silicon chips or ITO substrates of 1 cm^2 for AFM imaging. Silicon wafers were sonicated 15 min in acetone, rinsed with Milli-Q water, washed 30 min in piranha solution (3 : 1 of H$_2$SO$_4$ 98%/H$_2$O$_2$ 30% solution) and rinsed in Milli-Q water. The substrates were dried by spin-coating at a rotation rate at 2000 rpm during 20 s. ITO substrates of 1 cm^2 were washed 15 min in acetone and dried by spin coating at a rotation rate of 2000 rpm during 20 s. Filtered (0.2 μm PTFE) polymer solutions (10 mg of polymer per 1 mL of THF) were spin-coated at a rate of 2000 rpm during 40 s. The film thicknesses were determined by first scratching the film and then measuring the height profile by atomic force microscopy (AFM).

General procedure for the thermal annealing process. Samples were placed in a sealed glass case filled with argon. The case was left for 24 h in an oven at 200 °C.

General procedure for the rapid thermal annealing process. Rapid thermal annealing was performed inside a MILA-5000 heating unit with a nitrogen flux of 8 L min^{-1}. A ramp of 10 s

2 | *J. Mater. Chem. A*, 2015, **xx**, 1–7

This journal is © The Royal Society of Chemistry 2015

was applied in order to reach the target temperature (190 °C). A 60 s plateau was applied at the target temperature. Finally, the heating was stopped and the sample was cooled to 40 °C before opening the furnace.

General procedure for the solvent annealing process. Samples were placed in a glass case (135 mm diameter, 70 mm height) with two beakers containing 5 mL of solvent each. M beakers are 36 mm wide; L beakers are 45 mm wide. A weight is placed on the glass in order to keep the system hermetic. After the desired time the glass is removed in order to leave the samples to dry.

UV crosslinking. PTMA-*b*-PS thin films on ITO substrates were placed under three Rayonet photochemical reactor UV lamps emitting at 253 nm during 30 min. The distance to the lamps was about 3 cm.

Electrochemical measurements

Preparation of the Ag/Ag⁺ non-aqueous reference electrode. A non-aqueous Ag/Ag⁺ reference electrode with a porous Teflon tip was filled with a solution composed of 0.01 M $AgNO_3$ and 0.1 M $TBAClO_4$ in acetonitrile.

Typical procedure for cyclic voltammetry in solution. The analysed component (PTMA-*b*-PS or ferrocene) was dissolved into the electrolyte solution (0.1 M $TBAClO_4$ in acetonitrile) in order to obtain a 0.1 M solution. A three electrode setup with a Pt disk working electrode, a Pt wire counter electrode and the previously prepared Ag/Ag⁺ reference electrode was used to record the voltammogram.

Typical procedure for electrochemical characterisation of the PTMA-*b*-PS thin film on ITO substrates. Cyclic voltammetry was performed using a three electrode system with the PTMA-*b*-PS thin film deposited onto an ITO substrate as the working electrode, a Pt wire as the counter electrode and the previously prepared Ag/Ag⁺ reference electrode into 0.1 M $TBAClO_4$ in acetonitrile solution electrolyte.

Results and discussion

PTMA-*b*-PS block copolymer synthesis

PTMA-*b*-PS diblock copolymers were synthesized using a previously reported synthetic process.[28] In brief, a first block of PTMPM was polymerized by atom transfer radical

Table 1 Summary of PTMA-*b*-PS characteristic features

	M_n^a (g mol⁻¹)	$Đ_M^b$	PTMA ratio (weight%)	Degree of oxidation^c (%)
PTMA₃₂–PS₃₃₆	42 900	1.17	18	50
PTMA₄₂–PS₃₂₃	43 900	1.20	23	75
PTMA₅₆–PS₃₆₂	51 300	1.25	27	80
PTMA₇₉–PS₅₀₂	71 300	1.31	27	95
PTMA₄₂–PS₂₀₈	32 000	1.15	32	80
PTMA₄₂–PS₁₂₀	22 000	1.19	45	61

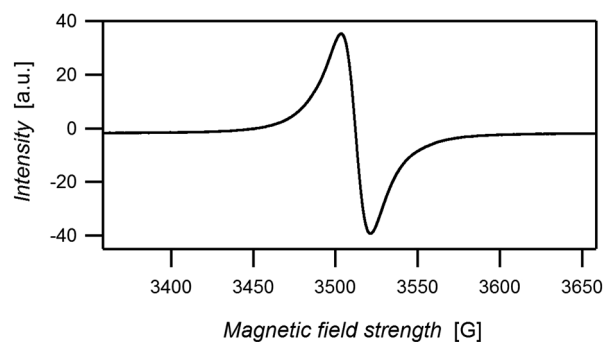^{a} Calculated from the ¹H NMR data. ^{b} Determined from GPC using PS standards. ^{c} Determined by ESR.

Fig. 1 ESR spectrum (X-band) of PTMA₃₂-*b*-PS₃₃₆.

polymerization (ATRP) and used as a macroinitiator for the formation of the PS block. Finally, the PTMPM block was oxidized into PTMA using *meta*-chloroperbenzoic acid (*m*CPBA). This controlled polymerisation technique leads to block copolymers with a controlled molar mass and narrow $Đ_M$. The characteristic features of the PTMA-*b*-PS further used for the self-assembly studies are described in Table 1. The degrees of polymerization (D_P) of the PTMPM and PS blocks were determined by ¹H-NMR. Number-averaged molar masses (M_n) were determined by gel permeation chromatography (GPC) using a PS calibration and the degrees of oxidation were determined by electron spin resonance (ESR) spectroscopy. The synthesized block copolymers show a degree of oxidation varying from 50 to 95%. The ESR spectra present a broad signal at 3512 G, which is typical for polymers bearing nitroxide radicals (Fig. 1).

Our objective is to obtain self-assembled thin films with cylinders of PTMA embedded in a PS matrix. Indeed, due to the solubility of PTMA in Li-ion battery electrolytes, a matrix of insoluble PS is suitable. Moreover, the PS matrix will add structural integrity to the cathode thin film. At the same time, continuity between the PTMA domains and the current collector is a prerequisite. According to these criteria cylindrical domains perpendicular to the current collector are preferred to spherical ones. It is generally admitted for block copolymer self-assembly processes in thin films that the cylindrical morphology is obtained upon using a block copolymer with a volume fraction (f_v) of the minor block comprised between 20 and 30%.[42,43] Due to the undetermined density of PTMA, f_v has been approximated to the mass ratio. According to this, the mass ratio of the PTMA block in the studied PTMA-*b*-PS block copolymers has been varied between 18 and 45 wt%.

Self-assembly of PTMA-*b*-PS in thin films

Thin films, with a thickness of approximately 80 nm, were prepared by spin coating PTMA-*b*-PS solutions (10 mg mL⁻¹) onto 1 cm² silicon chips. Phase separation is not always observed in the thin film after spin coating (Fig. 2a). Indeed, annealing procedures are often required in order to let the polymer chains to reorganize and reach a configuration closer to the thermodynamic equilibrium, increasing the phase separation.[26–29] The annealing thus allows for getting thin films showing better defined nanodomains in terms of size and
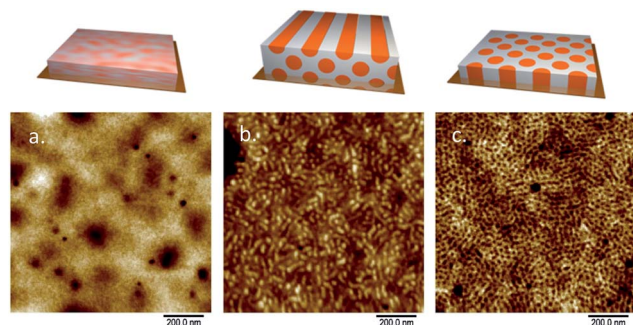
This journal is © The Royal Society of Chemistry 2015

J. Mater. Chem. A, 2015, **xx**, 1–7 | **3**

Fig. 2 AFM height images of PTMA$_{42}$-b-PS$_{323}$ thin films with 23 wt% of PTMA under different solvent annealing conditions during 6 h. (a) Thin film after spin coating without solvent annealing; (b) thin film after annealing with DEC (L) and H$_2$O (M); (c) thin film after annealing with DMF (L) and DEC (M).

shape, regularly distributed in the thin films with well-developed short and long range ordering. Furthermore, a careful control of the annealing conditions can allow the control of the orientation of the nanodomains in the thin films.[26–29] Two distinct annealing methods are mostly used to reach these goals. The first one, thermal annealing, consists of increasing the temperature of the thin films in order to overcome the glass transition (T_g) of the polymer blocks and hence to increase their mobility. The second one, solvent annealing, consists of exposing the thin films to vapours of good solvents for the polymer blocks in order to swell them and allow the mobility of polymer chains.

Both annealing techniques were investigated but thermal annealing as well as rapid thermal annealing[44] gave disappointing results (see ESI† section for further details). Solvent vapour annealing was investigated next. In the first step, different solvents were tested. It appears that the presence of two different solvents, each of them being placed in a distinct beaker in the controlled environment used for annealing (see the Experimental part), is more efficient than the use of one solvent alone. Best phase separation was obtained for the annealing realized in the presence of both dimethylformamide (DMF) and diethylcarbonate (DEC) (Fig. 2c). Indeed, DMF selectively swells the PS block while DEC is a selective solvent of the PTMA block. Therefore, mobility is imparted to both PS and PTMA chains during the

annealing process. Under such conditions, circular domains with an average diameter of 19 nm are visualized by AFM on top of the thin films. These domains could either correspond to spheres or to the apex of cylinders perpendicular to the film surface. However, due to the weight ratio of PTMA (23 wt%) in the starting block copolymer, they most likely correspond to perpendicularly oriented cylinders. Such a configuration is commonly observed in solvent annealed thin films with a cylindrical morphology and results from an alignment of the nanodomains with the solvent front as it evaporates at the end of the annealing process.[44–47] The cylindrical morphology in thin films can take two different orientations: parallel to the surface or perpendicular to the surface. The orientation is usually driven by the interfacial interactions between the polymer film and its surrounding, *e.g.* the film/substrate interface and the film/air (or solvent vapours) interface. The observed perpendicular orientation for annealing with DMF/DEC indicates that both blocks present the same interfacial interactions.[48] On the other side, solvent annealing with DEC/H$_2$O shows a cylindrical morphology with cylinders parallel to the surface (Fig. 2b). Since the film/substrate interface has not changed, the orientation shift can be attributed to the film/solvent vapour interface. Indeed, the PS selective solvent (DMF) has been changed for an unselective one (H$_2$O), changing the domain orientation. The annealing time is also recognized as a key factor.[49] Indeed, time is required to enable a good swelling of the polymer film, permitting PTMA and PS chains to move and rearrange. As shown in Fig. 3 an increase in annealing time results in an increase of the phase separation extent with at least 6 h of annealing needed to reach the optimum structuration. As expected, the weight ratio of PTMA in the copolymer is also an important parameter that allows tuning of the morphology in the thin film. In this respect, different morphologies, from spherical to lamellar, have been observed, depending on the weight ratio of PTMA. A higher PTMA weight ratio induces a lamellar morphology, as illustrated in Fig. 4, in which a fingerprint texture – typical to a lamellar morphology – is observed. Self-assembled morphologies are known to depend on two factors: the volume fraction (f_v), which has been discussed *via* the weight ratio structure dependence, and the Flory–Huggins parameter (χ). In the present study, the varying degree of oxidation (from 50 to 95%) is thought to influence the Flory–Huggins parameter. Indeed, PTMPM and PTMA are expected to have
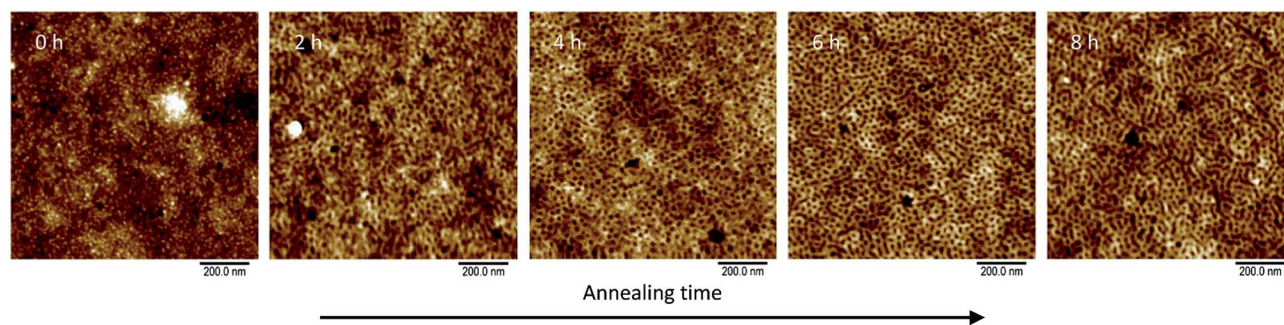

Fig. 3 AFM height images of PTMA$_{32}$-b-PS$_{336}$ thin films after annealing with DMF (L) and DEC (M) during different times. From no solvent annealing effect (left) to a strong solvent annealing effect after 8 h (right).
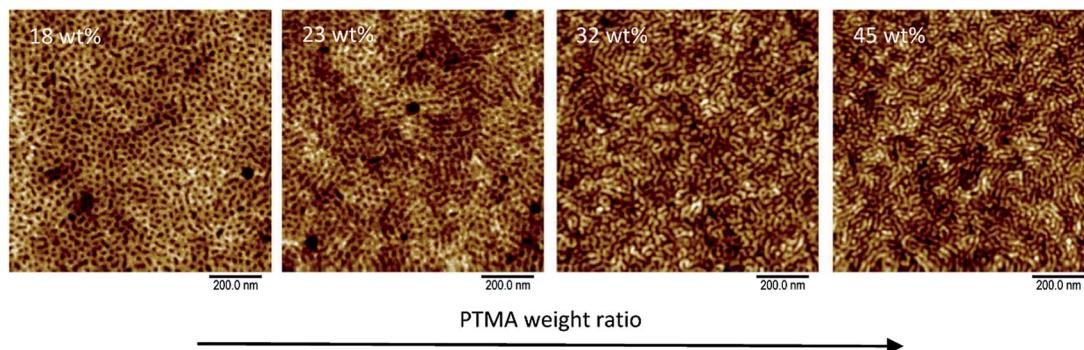
Fig. 4 AFM height images of PTMA-*b*-PS thin films with different weight ratios of PTMA after annealing with DMF (L) and DEC (M) during 6 h. See Table 1 for the polymer characteristic features.
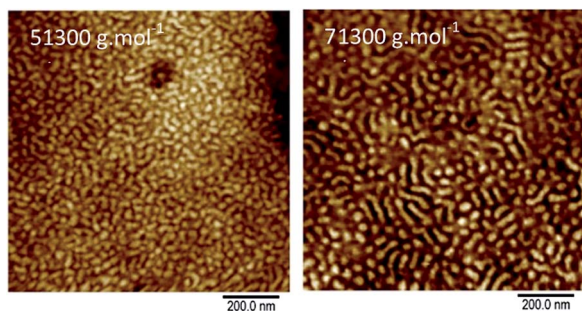

Fig. 5 AFM height images of PTMA-*b*-PS thin films with different M_n (indicated in the image in g mol^{-1}) for a same PTMA weight ratio of 27% after annealing with DMF (L) and DEC (M) during 6 h (L = 45 mm diameter beaker, M = 36 mm diameter beaker). See Table 1 for polymer characteristic features.

different polarities, *i.e.* χ parameters, and this should influence the extent of phase separation with the PS block. Therefore, it has to be kept in mind that the χ parameter is competing with the volume fraction during the self-assembly process.

The characteristic domain size is directly related to the total molar mass of the block copolymer. As shown in Fig. 5, the domains grow larger, the longer the copolymer is at a constant weight ratio. The estimated average size of the domains shifts from 20.9 nm for M_n = 51 300 to 29.7 nm for M_n = 71 300 g mol^{-1}, corresponding to an increase of 42% in domain size. Such an increase in domain size correlated with the D_P increase points out towards the strong segregation limit regime with $D_{éq}$ proportional to $N^{2/3}$.[50]

Finally, the influence of the substrate onto which the thin films have been prepared has been also investigated. Even if the detailed self-assembly study presented above was performed on silicon substrates, for electrochemical application, higher conductivities of the current collector are required. The change of the substrate from silicon to ITO minimally affects the self-assembly morphology.

Electrochemical analysis

The electrochemical tests were performed in a three electrode configuration with an Ag/Ag$^+$ non-aqueous reference electrode,

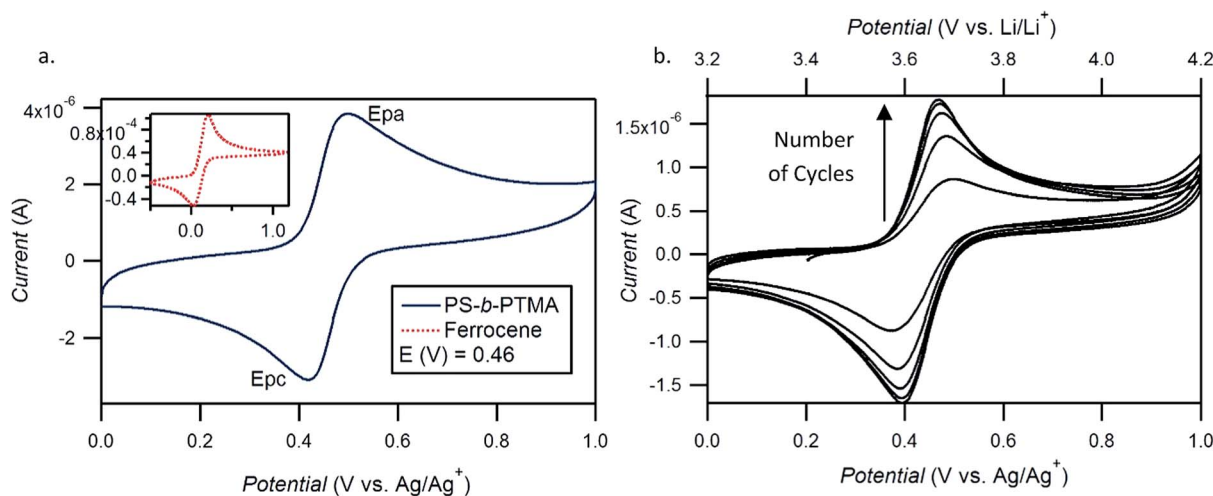**Fig. 6** Cyclic voltammogram of PTMA$_{79}$-*b*-PS$_{502}$ (0.1 mV s^{-1}; working = Pt disk (left) or ITO substrate (right); counter = Pt wire; ref. = Ag/Ag$^+$ (0.01 M AgNO$_3$ + 0.1 M TBAClO$_4$) electrolyte = 0.1 M TBAClO$_4$ in CH$_3$CN). (a) PTMA-*b*-PS in solution; (b) PTMA-*b*-PS thin film (potential *vs.* Li/Li$^+$ calculated).
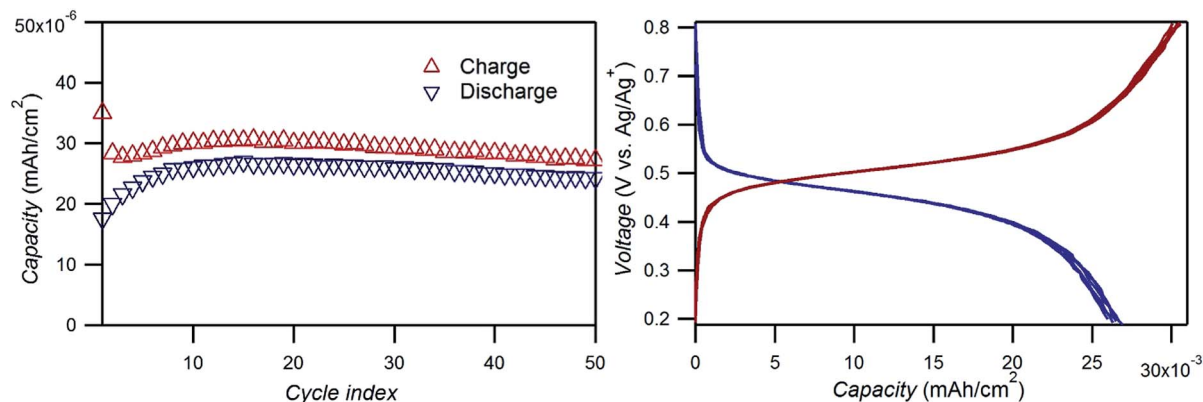
Fig. 7 Electrochemical characterization of a $PTMA_{79}$-*b*-PS_{502} thin film deposited onto an ITO substrate and cross-linked by UV for 45 min. Current applied: 23.7 μA cm^{-2}. Left: Capacity retention plot; right: charge/discharge voltage profile.

a Pt wire counter electrode and a solution of tetrabutylammonium perchlorate ($TBAClO_4$) in acetonitrile as the electrolyte.

First, the redox behaviour of PTMA-*b*-PS copolymers dissolved in acetonitrile was analysed by cyclic voltammetry. A pair of redox peaks centred at 0.46 V *vs.* Ag/Ag$^+$ and corresponding to the reversible oxidation of the free nitroxide radicals into oxoammonium cations was observed. Since the value of the redox potential against a Ag/Ag$^+$ reference electrode in organic media shifts depending on the solvent, electrolyte and concentration used, a calibration was required.[51] Ferrocene was used as an external standard and presents a potential of 0.11 V *vs.* used Ag/Ag$^+$ reference electrode (Fig. 6a). The potential of ferrocene has been reported to be *ca.* 3.22 V *vs.* lithium in carbonate-based electrolytes.[52] This gives us a potential of 3.57 V *vs.* Li/Li$^+$ for the PTMA-*b*-PS copolymers investigated here, which is coherent with values previously described in the literature.[7,8]

Cyclic voltammetry of a PTMA-*b*-PS thin film applied onto an ITO substrate was further performed. In order to avoid any dissolution of the thin film during electrochemical tests, the PS matrix was cross-linked by UV light irradiation at 253 nm during 30 min. The typical redox wave response of PTMA has been detected. The intensity of the measured current increases with the number of cycles, before reaching a maximum (Fig. 6b). This behaviour can be explained by a progressive swelling of the PS confined PTMA domains by the electrolyte upon cycling, allowing more electrochemically active sites to be reached.

Finally, constant current galvanostatic cycling tests have been performed on PTMA-*b*-PS thin films. A rapid charge/discharge process was required in order to avoid self-discharge, which was observed at a slower rate. Indeed, due to the reduced amount of active material present in a thin film compared to its high surface, self-discharge is a challenging issue. The capacity retention plot shows a good retention of capacity over time (Fig. 7). Similar to cyclic voltammetry experiments, an increase in capacity is observed during the first cycles and is attributed to the swelling of the thin film by the electrolyte. Charge/discharge profiles reveal a plateau around 0.48 V *vs.* Ag/Ag$^+$ in both charge and discharge which is coherent

with the PTMA behaviour and a requirement for battery application in order to deliver a constant voltage.

Conclusions

A nanostructured organic radical cathode was prepared by the self-assembly of PTMA-*b*-PS diblock copolymers in thin films. In order to control the phase separation morphology, the effect of thermal and solvent annealing was investigated. Thermal annealing appeared to be inefficient; therefore, solvent annealing was used and resulted in the formation of thin films with different morphologies such as lamellar or cylindrical. PTMA-*b*-PS thin films with perpendicularly oriented cylinders of PTMA inside a PS matrix were further investigated. Thanks to the UV crosslinked PS matrix, PTMA dissolution into the battery electrolyte was avoided and enhanced mechanical integrity of the cathode is expected. At the same time, perpendicularly oriented PTMA cylinders allow continuity between the electrochemical active moieties and the ITO current collector. The choice of the solvent used for annealing is a key parameter in order to obtain the desired morphology. The simultaneous use of DMF and DEC gave the best results for our system. The electrochemical activity of PTMA-*b*-PS using a three electrode setup has been demonstrated. Cyclic voltammetry of the polymer in solution and in the thin film was recorded displaying the typical behaviour of PTMA. In thin films, charge/discharge measurements and capacity retention plot were also performed. This work opens a new field of research on ORBs using block copolymers. Indeed, nano-batteries can find applications in microelectronic devices. Even if the PS is an electrochemically inactive material, this work paves the way towards other block copolymers where the PS moiety can be replaced by another material allowing a synergy with PTMA, such as a conductive polymer.

Acknowledgements

Notes and references

1 Y. Liang, Z. Tao and J. Chen, *Adv. Energy Mater.*, 2012, **2**, 742–769.

2 T. Janoschka, M. D. Hager and U. S. Schubert, *Adv. Mater.*, 2012, **24**, 6397–6409.

3 M. Suguro, A. Mori, S. Iwasa, K. Nakahara and K. Nakano, *Macromol. Chem. Phys.*, 2009, **210**, 1402–1407.

4 M. Armand and J.-M. Tarascon, *Nature*, 2008, **451**, 652–657.

5 K. Oyaizu and H. Nishide, *Adv. Mater.*, 2009, **21**, 2339–2344.

6 K. Nakahara, S. Iwasa, M. Satoh, Y. Morioka, J. Iriyama, M. Suguro and E. Hasegawa, *Chem. Phys. Lett.*, 2002, **359**, 351–354.

7 H. Nishide, S. Iwasa, Y.-J. Pu, T. Suga, K. Nakahara and M. Satoh, *Electrochim. Acta*, 2004, **50**, 827–831.

8 H. Nishide and T. Suga, *Electrochem. Soc. Interface*, 2005, 32–36, Winter.

9 K. Nakahara, J. Iriyama, S. Iwasa, M. Suguro, M. Satoh and E. Cairns, *J. Power Sources*, 2007, **165**, 870–873.

10 K. Nakahara, J. Iriyama, S. Iwasa, M. Suguro, M. Satoh and E. Cairns, *J. Power Sources*, 2007, **163**, 1110–1113.

11 K. Nakahara, J. Iriyama, S. Iwasa, M. Suguro, M. Satoh and E. Cairns, *J. Power Sources*, 2007, **165**, 398–402.

12 H. Li, Y. Zou and Y. Xia, *Electrochim. Acta*, 2007, **52**, 2153–2157.

13 A. Vlad, N. Singh, J. Rolland, S. Melinte, P. M. Ajayan and J.-F. Gohy, *Sci. Rep.*, 2014, **4**, 4315.

14 A. Vlad, J. Rolland, G. Hauffman, B. Ernould and J.-F. Gohy, *ChemSusChem*, 2015, **1348**, DOI: 10.1002/cssc.201500246.

15 T. Suga, S. Takeuchi, T. Ozaki, M. Sakata, K. Oyaizu and H. Nishide, *Chem. Lett.*, 2009, **38**, 1160–1161.

16 Y. Yonekuta, T. Kurata and H. Nishide, *J. Photopolym. Sci. Technol.*, 2005, **18**, 39–40.

17 T. Sukegawa, A. Kai, K. Oyaizu and H. Nishide, *Macromolecules*, 2013, **46**, 1361–1367.

18 K. Nakahara, K. Oyaizu and H. Nishide, *Chem. Lett.*, 2011, **40**, 222–227.

19 U. S. Schubert, *Polymer*, 2015, **68**, 308–309.

20 P. Nesvadba, L. Bugnon, P. Maire and P. Novák, *Chem. Mater.*, 2010, **22**, 783–788.

21 E. P. Tomlinson, M. E. Hay and B. W. Boudouris, *Macromolecules*, 2014, **47**, 6145–6158.

22 T. Suga, Y.-J. Pu, S. Kasatori and H. Nishide, *Macromolecules*, 2007, **40**, 3167–3173.

23 B. T. Suga, H. Ohshiro, S. Sugita, K. Oyaizu and H. Nishide, 2009, **8555**, 1627–1630.

24 T. Suga, S. Sugita, H. Ohshiro, K. Oyaizu and H. Nishide, *Adv. Mater.*, 2011, **23**, 751–754.

25 T. Suga and H. Nishide, *ACS Symp. Ser.*, 2012, **1096**, 45–53.

26 T. Jähnert, T. Janoschka, M. D. Hager and U. S. Schubert, *Eur. Polym. J.*, 2014, **61**, 105–112.

27 T. Janoschka, A. Teichler, A. Krieg, M. D. Hager and U. S. Schubert, *J. Polym. Sci., Part A: Polym. Chem.*, 2012, **50**, 1394–1407.

28 G. Hauffman, J. Rolland, J.-P. Bourgeois, A. Vlad and J.-F. Gohy, *J. Polym. Sci., Part A: Polym. Chem.*, 2013, **51**, 101–108.

29 T. Sukegawa, H. Omata, I. Masuko, K. Oyaizu and H. Nishide, *ACS Macro Lett.*, 2014, **3**, 240–243.

30 L. Rostro, A. G. Baradwaj and B. W. Boudouris, *ACS Appl. Mater. Interfaces*, 2013, **5**, 9896–9901.

31 H. C. Lin, C. C. Li and J.-T. Lee, *J. Power Sources*, 2011, **196**, 8098–8103.

32 C. H. Lin, W. J. Chou and J. T. Lee, *Macromol. Rapid Commun.*, 2012, **33**, 107–113.

33 Y.-H. Wang, M.-K. Hung, C.-H. Lin, H.-C. Lin and J.-T. Lee, *Chem. Commun.*, 2011, **47**, 1249–1251.

34 B. Ernould, M. Devos, J.-P. Bourgeois, J. Rolland, A. Vlad and J.-F. Gohy, *J. Mater. Chem. A*, 2015, DOI: 10.1039/c5ta00570a.

35 K. Takahashi, K. Korolev, K. Tsuji, K. Oyaizu, H. Nishide, E. Bryuzgin, A. Navrotskiy and I. Novakov, *Polymer*, 2015, **68**, 310–314.

36 T. Suga, S. Takeuchi and H. Nishide, *Adv. Mater.*, 2011, **23**, 5545–5549.

37 X. Zhuang, C. Xiao, K. Oyaizu, N. Chikushi, X. Chen and H. Nishide, *J. Polym. Sci., Part A: Polym. Chem.*, 2010, **48**, 5404–5410.

38 G. Hauffman, Q. Maguin, J.-P. Bourgeois, A. Vlad and J.-F. Gohy, *Macromol. Rapid Commun.*, 2014, **35**, 228–233.

39 L. Rostro, A. G. Baradwaj, A. R. Muller, J. S. Laster and B. W. Boudouris, *MRS Commun.*, 2015, DOI: 10.1557/mrc.2015.27.

40 T. Suga, M. Sakata, K. Aoki and H. Nishide, *ACS Macro Lett.*, 2014, **3**, 703–707.

41 C. Liedel, A. Moehle, G. D. Fuchs and C. K. Ober, *MRS Commun.*, 2015, DOI: 10.1557/mrc.2015.50.

42 G. H. Fredrickson and F. S. Bates, *Annu. Rev. Mater. Sci.*, 1996, **26**, 501–550.

43 F. Bates, *Science*, 1991, **251**, 898–905.

44 K. Fukunaga, H. Elbs, R. Magerle and G. Krausch, *Macromolecules*, 2000, **33**, 947–953.

45 K. Fukunaga, T. Hashimoto, H. Elba and G. Krausch, *Macromolecules*, 2003, **36**, 2852–2861.

46 G. Kim and M. Libera, *Macromolecules*, 1998, **31**, 2569–2577.

47 S. H. Kim, M. J. Misner, T. Xu, M. Kimura and T. P. Russell, *Adv. Mater.*, 2004, **16**, 226–231.

48 G. and Nealey, *Directed Self-assembly of Block Copolymers for Nano-manufacturing*, WoodHead Publishing, 1st edn, 2015.

49 S. Park, B. Kim, J. Xu, T. Hofmann, B. Ocko and T. Russell, *Macromolecules*, 2009, **42**, 1278–1284.

50 J. K. Kim, S. Y. Yang, Y. Lee and Y. Kim, *Prog. Polym. Sci.*, 2010, **35**, 1325–1349.

51 V. V. Pavlishchuk and A. W. Addison, *Inorg. Chim. Acta*, 2000, **298**, 97–102.

52 C. O. Laoire, E. Plichta, M. Hendrickson, S. Mukerjee and K. M. Abraham, *Electrochim. Acta*, 2009, **54**, 6560–6564.